



Structural Insights into the Role of Diphthamide on Elongation Factor 2 in mRNA Reading-Frame Maintenance

Simone Pellegrino¹, Natalia Demeshkina¹, Eder Mancera-Martinez², Sergey Melnikov¹, Angelita Simonetti², Alexander Myasnikov¹, Marat Yusupov^{1,3}, Gulnara Yusupova¹ and Yaser Hashem⁴

1 - Department of Integrated Structural Biology, Institute of Genetics and Molecular and Cellular Biology, CNRS UMR710, INSERM U964, University of Strasbourg, Strasbourg 67000, France

2 - Architecture and Reactivity of RNA, University of Strasbourg, Institute of Molecular and Cellular Biology of the CNRS UPR9002, Strasbourg 67084, France

3 - Institute of Fundamental Medicine and Biology, Kazan Federal University, Kazan 420008, Russia

4 - ARNA, U1212 Université de Bordeaux, Institut Européen de Chimie et de Biologie (IECB) Inserm, Pessac 33600, France

Correspondence to Marat Yusupov, Gulnara Yusupova and Yaser Hashem: M. Yusupov and G. Yusupova are to be contacted at: Institut de Génétique et de Biologie Moléculaire et Cellulaire (IGBMC), 1 rue Laurent Fries/BP 10142/67404 Illkirch Cedex, France; Y. Hashem is to be contacted at: Institut Européen de Chimie et de Biologie (IECB), 2 Rue Robert Escarpit, 33600 Pessac, France. marat@igbmc.fr; gula@igbmc.fr; yaser.hashem@u-bordeaux.fr
<https://doi.org/10.1016/j.jmb.2018.06.006>

Edited by Ruben L. Gonzalez

Abstract

One of the most critical steps of protein biosynthesis is the coupled movement of mRNA, which encodes genetic information, with tRNAs on the ribosome. In eukaryotes, this process is catalyzed by a conserved G-protein, the elongation factor 2 (eEF2), which carries a unique post-translational modification, called diphthamide, found in all eukaryotic species. Here we present near-atomic resolution cryo-electron microscopy structures of yeast 80S ribosome complexes containing mRNA, tRNA and eEF2 trapped in different GTP-hydrolysis states which provide further structural insights into the role of diphthamide in the mechanism of translation fidelity in eukaryotes.

© 2018 Elsevier Ltd. All rights reserved.

Introduction

During protein synthesis, mRNA and tRNA move in a coordinated and accurate way along the ribosome. In eukaryotes, this complex process of translocation is ensured by a translational GTPase, elongation factor 2 (eEF2), which is homologous to bacterial elongation factor EF-G [1]. According to structural and biochemical experiments, after peptidyl transfer reaction, the small ribosomal subunit (SSU) spontaneously rotates relative to the large ribosomal subunit (LSU). This rotation results in the movement of acceptor ends of tRNAs on LSU to P and E site while leaving main bodies of tRNAs bound to the A and P sites of SSU (A/P and P/E hybrid states, respectively) (see a review in Ref. [2]). In addition to this intersubunit ratcheting-like motion, large conformational changes occur inside SSU by itself. Thus, swivelling of the head domain and rearrangement of the shoulder promote

further movement of tRNAs on SSU from their A and P sites to the P and E sites. These rearrangements are coordinated and catalyzed by eEF2, which hydrolyzes GTP and controls the precise movement of mRNA with tRNA through multiple intermediate states.

Main structural knowledge about dynamics of the eukaryotic elongation cycle, in the presence of mRNA and tRNA, has been provided by low to intermediate-resolution cryo-electron microscopy (cryo-EM) reconstructions that enabled the understanding of the major conformational rearrangements responsible for guiding the translocation process [3–5]. These snapshots were captured in different GTP hydrolysis states and suggested that eEF2 binds to a ratcheted ribosome as was originally discovered in bacteria (see a review in Ref. [2]). Notwithstanding, due to the limited resolutions obtained by these reconstructions, a detailed structural understanding of the mechanism by which eEF2 catalyzes translocation in eukaryotes remained

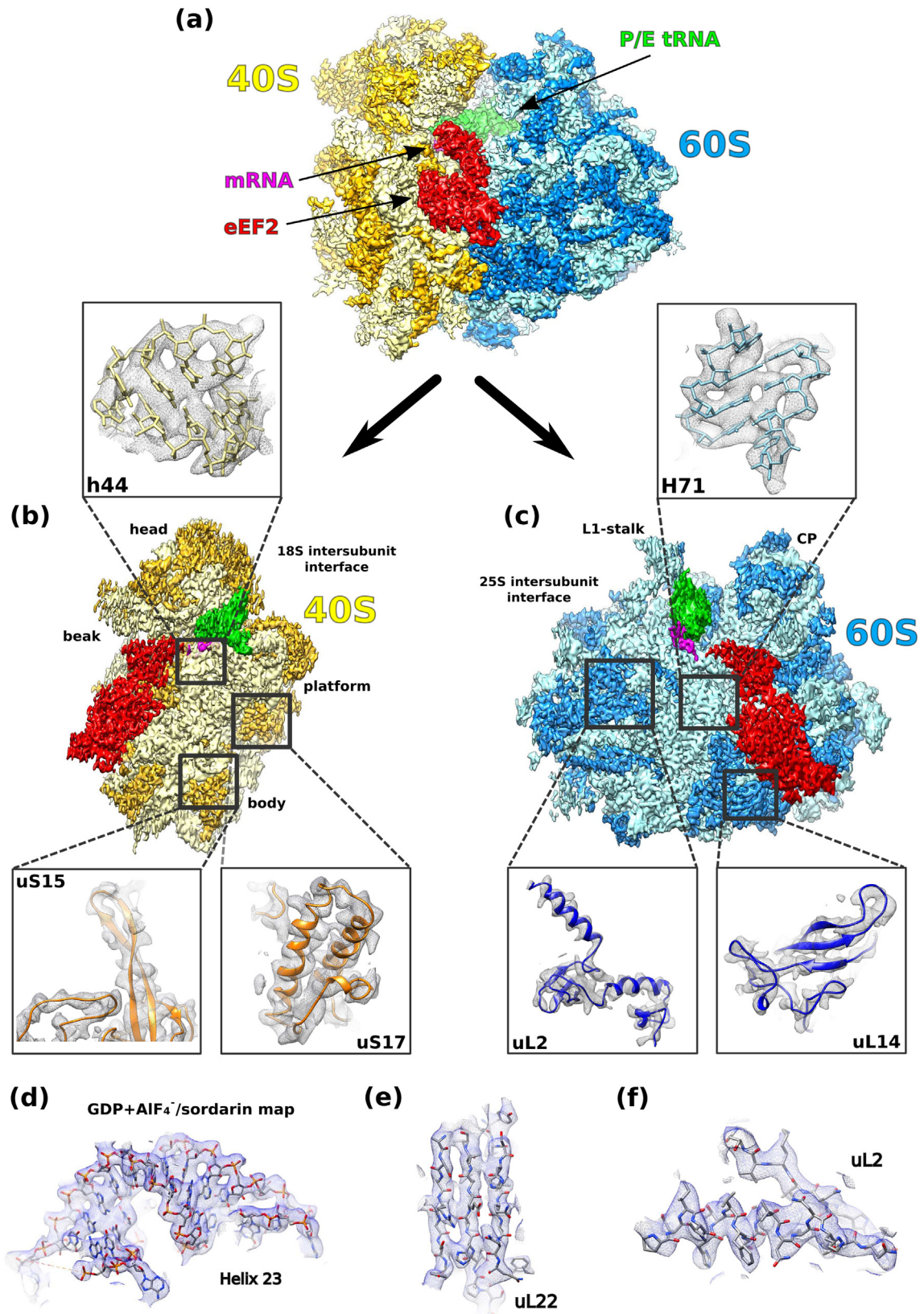


Fig. 1 (legend on next page)

unclear. eEF2 is well conserved among eukaryotes and it carries a unique post-translational modification, covalently bound to a conserved histidine residue (His699 in yeast) and called diphthamide, which is absent in bacteria [6, 7]. Diphthamide is targeted by at least two virulent toxins—diphtheria toxin and *Pseudomonas aeruginosa* exotoxin A—which transfer ADP ribose to the modification and inactivate eEF2 leading to cell death [7]. Diphthamide biosynthesis is accomplished by a set of highly conserved proteins: yeast strains lacking these enzymes display increased mRNA frame-shifting, pointing to a crucial role of the modification in protein synthesis fidelity [6]. Furthermore, in mammals, defects in the diphthamide synthesis can lead to certain neurodegenerative diseases [8]. Consequently, in order to better understand how diphthamide regulates ribosomal translocation, there is an evident need for structures at higher resolution.

Here we present near-atomic resolution reconstructions, obtained by cryo-EM, of eukaryotic 80S ribosomes, containing eEF2 in different hydrolytic states, tRNA and mRNA, providing new insights into the role that the eukaryotic-specific unique post-translational modification diphthamide might have in ensuring correct mRNA reading frame. This study has enabled us to visualize in details the direct involvement of diphthamide with the mRNA in the context of translocating ribosomes.

Results and Discussions

Near-atomic resolution structures of ribosomes in an intermediate step of translocation

To understand more deeply the role of diphthamide in ribosomal translocation, we solved three near-atomic resolution cryo-EM structures of yeast 80S/tRNA/mRNA/eEF2 complexes trapped in different GTP-hydrolysis states. “GMPPCP complex” was formed using 80S ribosomes from *Saccharomyces cerevisiae*, 24 nucleotides long mRNA containing 3 consecutive phenylalanine codons, cognate yeast tRNA^{Phe}_{GAA}, native eEF-2 from *S. cerevisiae* and GMPPCP, a non-hydrolyzable analog of GTP. The “GMPPCP complex” was reconstructed at 3.8 Å (Figs. 1, 2a–e, and 3a–b; Supplement Figs. 1 and 2a). The second 80S complex, “AlF₄⁻/sordarin

complex,” was formed by addition of GDP and aluminium fluoride (AlF₄⁻) instead of GMPPCP. In addition, we added the drug sordarin, which specifically targets fungal eEF2 preventing its release from the ribosome [10]. Previously, it was shown that AlF₄⁻ mimics the γ-phosphate of GTP [11] during hydrolysis in GTPases. Thus, GDP-AlF₄⁻ presumably traps 80S ribosome-bound eEF-2 in a transition-like state of GTP hydrolysis in the present complex. The “AlF₄⁻/sordarin complex” was reconstructed at 3.7 Å (Figs. 2f–i and 3c–d, and Supplement Figs. 1 and 2b). The third 80S ribosome complex, “GMPPCP/sordarin complex,” was formed as it was described above for “GMPPCP complex,” but in the presence of sordarin. This complex was designed to provide understanding of the drug when eEF2 is bound to the ribosome in a GTP-like state. The “GMPPCP/sordarin complex” was reconstructed at 4.30-Å average resolution (Figs. 2j–m and 3e–f, and Supplement Figs. 1 and 2c).

In order to obtain the most homogeneous population for each complex, we performed several rounds of 3D sorting. 3D refinement jobs in RELION [12], with or without user-defined masks (Experimental procedures, Supplement Fig. 1), thus cover the whole 80S (along with eEF2, tRNA and mRNA), the SSU (along with eEF2, tRNA and mRNA), or the LSU (along with the most stable regions of the SSU at its intersubunit side, eEF2, tRNA and mRNA), respectively. These local refinements were performed to allow for better alignment of the particles around the regions of interest, leading to higher-resolution reconstructions with a better-resolved ribosomal core (Fig. 1 and Supplement Fig. 1). In spite of our efforts in improving the resolution of our reconstructions, the local resolution of eEF2, especially for domain IV, represents a real bottleneck and persisted in a range between 4 and 4.5 Å (Supplement Fig. 1). High level of flexibility of domain IV of eEF2 bound to the ribosome was previously reported [3–5]. More generally, compared to the 60S local resolution, it appears that eEF2 keeps a certain level of flexibility around the observed global conformations. This is due to the fact that the SSU adopts a continuum of subtle conformations around its observed rotated state, which in turn impacts the stability of eEF2, thus limiting the resolutions of our complexes for the latter. Such a continuum of the SSU movements around an average optimal position is a usual and persistent problem in

Fig. 1. Reconstruction maps allowed to interpret features at high resolution. (a) Top view of the “GMPPCP complex” taken from the GTPase reaction center with eEF2, P/E tRNA and mRNA indicated. (b) View of the SSU from the 18S rRNA intersubunit interface. eEF2, mRNA and tRNA are shown. In the zoomed-in square details of rRNA, α-helices and β-strands (shown in cartoon for proteins) are shown. (c) View of the LSU from the 25S rRNA intersubunit interface, with details of the structure fitted (shown as cartoon for proteins) into the density map. CP: central protuberance. (d–f) Zoom-in of rRNA, β-strands and α-helices of the “AlF₄⁻/sordarin complex” fitted into density. The overall quality of the map displays high resolution features, as single-nucleotide bases (rRNA) and side chains (proteins). Residues are shown as sticks for a better representation.

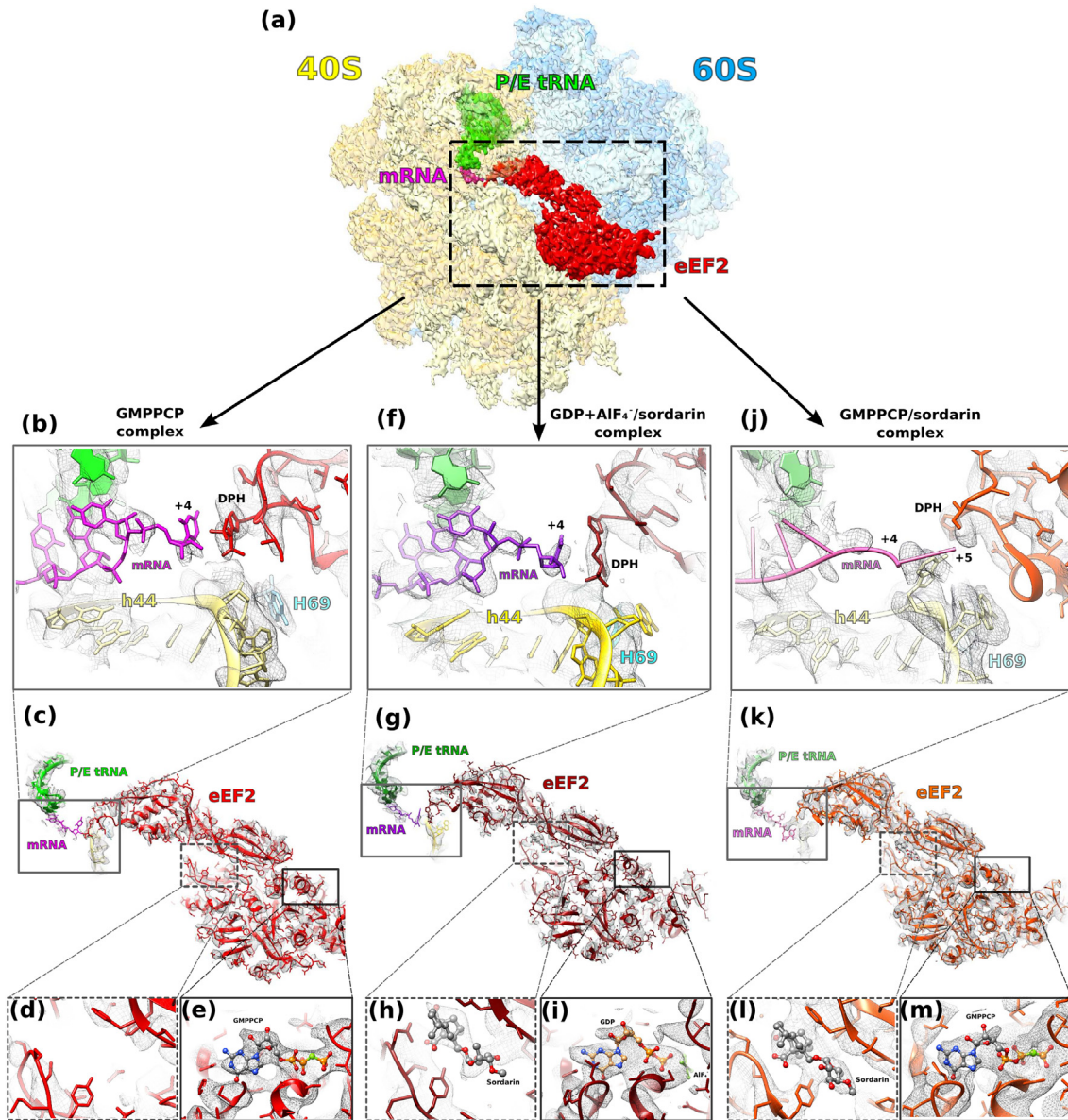


Fig. 2. Structural analysis of the three complexes representing an intermediate state of eEF2 catalyzed translocation. (a) Top view of *Saccharomyces cerevisiae* 80S ribosome in complex with eEF2 (red), P/E site tRNA (green) and mRNA (magenta). (b, d, j) Close-up views of the decoding region for the three complexes analyzed in this study. The diphthamide modification of eEF2 in the “GMPPCP complex” interacts with the mRNA in position +4 (“inward” conformation) (b), while in the presence of the drug sordarin, it points away from the DC (“outward”) (j). For the transition state complex (GDP + AIF₄⁻), diphthamide is adopting an alternative conformation and it points again toward h44 on the SSU (f). SSU-focused map “AIF₄⁻/sordarin complex” has been used for this representation, since it allowed for better interpretation of the density corresponding to eEF2 and diphthamide. tRNA and part of domain IV of eEF2 are also shown into density for all the complexes. In panel j, the mRNA was represented in ribbons to highlight the relatively modest interpretability of the mRNA density compared to the other two complexes, probably as a consequence of the weak interaction with the diphthamide because of its very different conformation. (c, g, k) A section through the eEF2 fitted into its density maps. The three analyzed complexes in this study are colored consistently but with different tones in order to differentiate them from each other. tRNAs and mRNAs are shown as fitted into density. (d, e) Zoom on the sordarin and the nucleotide-binding pockets, respectively, for the “GMPPCP complex.” (h, i) Same as panels d and e but for the “AIF₄⁻/sordarin complex.” (l, m) Same as panels d and e but for the “GMPPCP/sordarin complex.” DPH, diphthamide.

most of reported cryo-EM studies of various ribosomal complexes. More extensive 3D particle sorting did not solve the SSU flexibility issue, probably because of

the continuous nature of the subtle moments around the observed conformation. However, as it is described and supported by our figures herein, the

quality of our maps is sufficient to resolve the different conformations of the diphthamide modification and provide insightful structural understanding of its engagement in ribosomal translocation (Figs. 1–4, and Supplement Figs. 3 and 4). Because of the consistent limited resolution of eEF2 (comprised between 4 and 4.5 Å) among our three complexes in spite of their different global resolutions, which is due to their inherent flexibility, we did not attempt improving the resolution by collecting more data.

Our reconstructions reveal that the tRNA binds in the P/E hybrid state, by superposition with the structure of a rotated 80S•tRNA ribosome [13] (PDB: 3j77) (Fig. 1, 2a, and 3, and Supplement Fig. 5a). However, we observe a more extended anti-clockwise head swivelling of $\sim 9.5^\circ$ (<http://rna.ucsc.edu/macenter/erodaxis.py>) [14] (Supplement Fig. 5b), similar to the yeast

80S/eEF2 complex in the presence of Taura syndrome virus (TSV) IRES (PDB: 5juu; Supplement Fig. 5b), where the SSU is proposed to be fully rotated [15]. To obtain the closest to physiologically relevant *in vitro* complexes, we did not use any A-site tRNA-stabilizing drug (see a review in Ref. [2]), such as aminoglycosides or tuberactinomycins. The accommodation of tRNA in the P/E hybrid state is mainly driven by the ratchet-like subunit rotation (RSR) that we and others observed [3]. Although our mRNA construct was designed to accommodate a tRNA in the A-site, we did not observe any density for it in our reconstructions. This is likely due to the low affinity that deacylated tRNA has for the A-site, and to the fact that the simultaneous binding of A-tRNA and eEF2 in GTP-like state to the ribosome results in a highly dynamic and transient state [16]. Structural comparison with

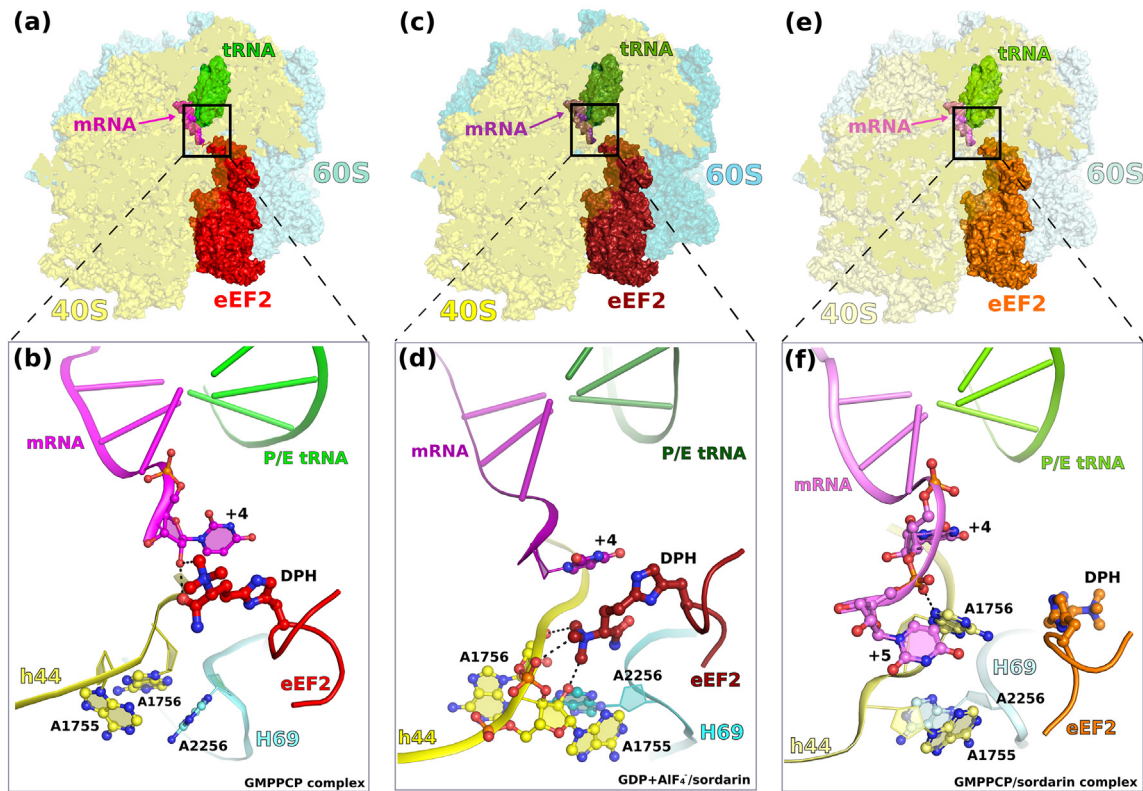


Fig. 3. Diphthamide interactions within the reported translocating 80S complexes at different GTP-hydrolytic states. (a, c, e) Transverse sections of the cryo-EM maps of the “GMPPCP” (a), “AlF₄⁻/sordarin” (c) and “GMPPCP/sordarin” (e) ribosomal complexes. (b, d, f) Atomic model of the DC from the different reported translocating complexes, highlighting the interacting network of diphthamide. In the “GMPPCP complex” (b), the diphthamide interacts with the sugar moiety of mRNA in position +4, while the conserved residues of the DC (A1755 and A1756) are both flipped-in the minor groove of h44. The presence of sordarin induces the diphthamide to adopt the “inward” conformation [“GMPPCP/sordarin complex” (f)]. This in turn induces A1756 to flip-out as for interacting with the mRNA, similarly to what observed for bacterial 70S/mRNA/2tRNAs (Jenner *et al.* [9]). When GTP is hydrolyzed, but the γ -phosphate has not been released yet, the tip of eEF2 domain IV and the DC residues rearrange in an intermediate conformation (d). In this case, the diphthamide interacts with the sugar-backbone of A1755/56 and it is facing to the mRNA in position +4. The mRNA (tones of magenta), tRNA (tones of green), the diphthamide-containing loop of eEF2 (tones of red), the decoding SSU rRNA nucleotides (tones of yellow) and the tip of H69 (tones of cyan) are indicated. DPH, diphthamide.

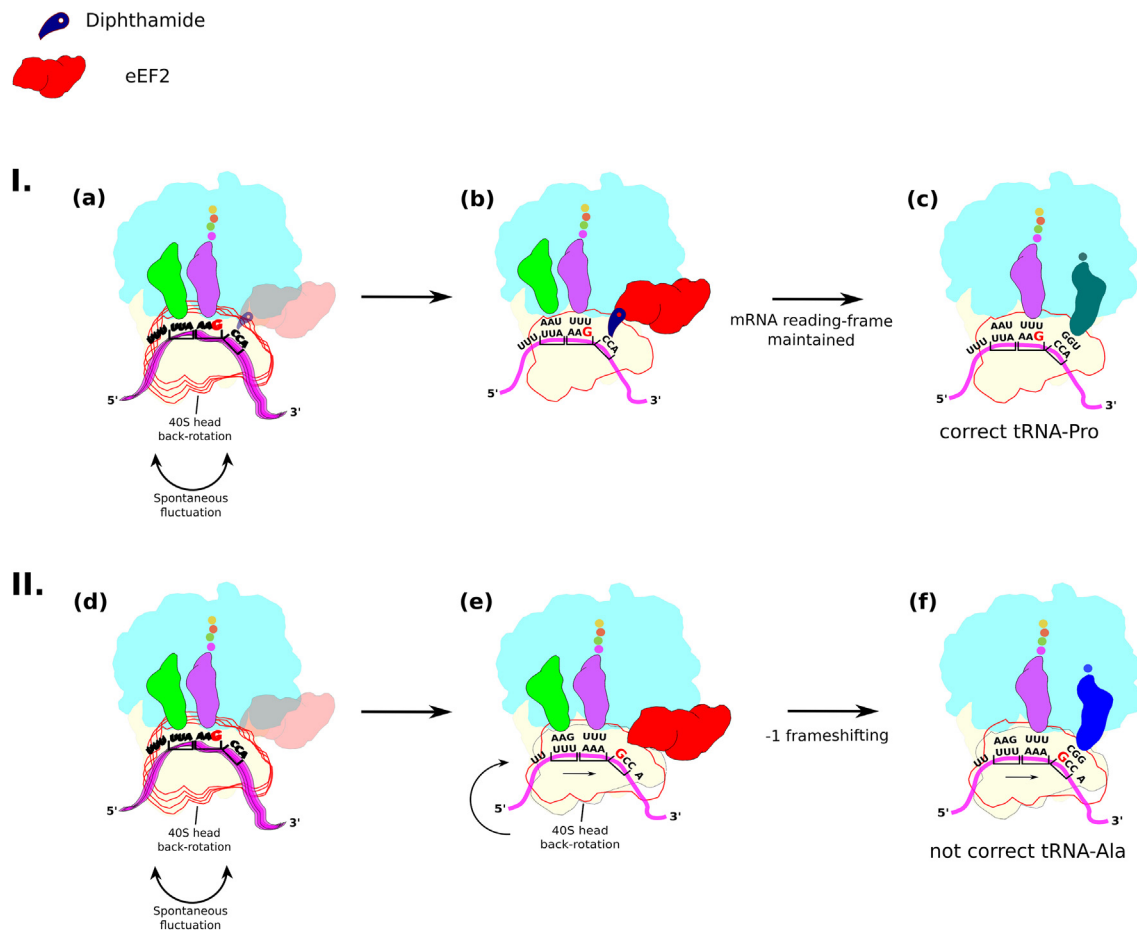


Fig. 4. Proposed mechanism of action of diphthamide during ribosomal translocation in eukaryotes. Ribosomal translocation involves the concerted movement of mRNA and tRNA along the ribosome. The SSU plays a major role in this mechanism through overall rotation (ratcheting) and movement of the head domain (swivelling). eEF2 is the main actor in catalysis of these steps. Our data suggest that eEF2 is not only doing so. We observe that a complex network of interactions involving the mRNA, the DC residues and the diphthamide, depending on the hydrolytic state and the presence or absence of the inhibitor sordarin, is formed upon eEF2 binding (Fig. 3). The “GMPPCP” and “AIF₄/sordarin” complexes are relevant for understanding, into more details, the structural role of the unique modification diphthamide (I). Even in the presence of eEF2, the head domain of the SSU is a flexible entity that can undergo spontaneous fluctuations, which in turn might lead to the slippage of mRNA (eEF2 is represented in shadow for clarity) (a). The structure we obtain reveals that eEF2 might prevent the head domain to back-rotate by binding directly to the mRNA via diphthamide, and more specifically at the residue in +4 position (b). In turn, this interaction might keep the correct reading frame of the mRNA and allow for the loading of the correct aminoacylated-tRNA once translocation has finished (c). However, when diphthamide is not expressed or the tip of domain IV is not properly folded (II), it has been shown biochemically that –1 frameshifting events occur with higher frequency [6]. Thus, most likely, the deficient eEF2 is not able to prevent back-rotation of the head of the SSU (d), which in turn might cause mRNA frameshift and load the non-correct aminoacylated-tRNA or introduce premature stop codons (e, f).

bacterial 70S/tRNA/mRNA/EF-G complexes in the presence of GMPPCP (PDB: 4v90 and 4v9H) also confirmed that our structures are representatives of intermediate states of translocation [17, 18] (Supplement Fig. 6). We also found that in our complexes, a further displacement of ~7 Å of the tRNA elbow takes place, coupled with a movement of the L1-stalk toward the LSU (Supplement Fig. 6a). This state likely corresponds to one of the first intermediates of the “unlocked” ribosome induced by eEF2 [15].

The binding of diphthamide to mRNA at position +4 appears to be crucial for translation fidelity

The molecular mechanism by which diphthamide participates in ribosomal translocation is highly complex and the recent structures represent only one hydrolytic state of eEF2 [15, 19]. Analysis of “GMPPCP complex” shows that diphthamide of eEF2 is pointing toward the mRNA path (“outward” state) and interacts with its sugar-backbone moiety at position +4

(Figs. 2b, 3b, and 4, and Supplement Figs. 3a–c and 4a). The position of the tip of domain IV, and consequently of the diphthamide, relative to the mRNA suggests that, when eEF2 is bound to the 80S ribosome in the GTP-like state, diphthamide might function as a “pawl” preventing slippage or frame-shifting of mRNA, hence ensuring the fidelity of translocation as proposed earlier, as well as in bacteria [3, 20, 21].

Intersubunit bridge B2a, mainly composed of the top of helix 44 (h44) in the SSU and the apical loop of helix 69 (H69) in the LSU [3, 22], plays a pivotal role in ribosomal translocation [3]. In spite of the fact that overall conformation of the B2a region does not change significantly when compared to bacteria (Supplement Fig. 6b), the close-up view of the decoding nucleotides A1755/56 (A1492/93 in *Escherichia coli*) of 18S rRNA and A2256 (A1913 in *E. coli*) of 25S rRNA reveals several remarkable rearrangements (Fig. 3). In the “GMPPCP complex,” for instance, A1755 and A1756 reside inside the minor groove of h44 (flip-in) with A2256 of H69 located outside of the groove and stabilized by interactions with A1756 (Figs. 2b and 3b).

In the cryo-EM reconstruction of the “AIF₄/sordarin complex,” in which eEF2 is trapped in a transition-like state after GTP hydrolysis (Figs. 2f and 3d, and Supplement Figs. 2b and 4b), diphthamide points toward the DC and interacts with the sugar-phosphate backbone of decoding nucleotides A1755/56. In this complex, A1756 is in a flipped-in intermediate conformation as compared to the “GMPPCP complex” (Fig. 3b, d, and Supplement Figs. 2a–b and 3d–f), while A1755 adopts a different conformation. Both residues of the decoding center (DC) create a network of interactions with the tip of H69, precisely residue A2256. The conformational change of A1755 likely impedes A1756 to flip-in completely as seen for the “GMPPCP complex” (Fig. 3).

Sordarin induces a different conformation of diphthamide in the GTP-like state

Sordarin is known to bind to domain III of fungal eEF2 (Fig. 2h and i) and suggested to prevent release of eEF2 from the ribosome [10]. In the “GMPPCP/sordarin complex,” diphthamide flips 180° toward eEF2, adopting an alternative conformation, which we termed “inward” (Figs. 2j and 3e–f, and Supplement Figs. 2c and 3g–i), with A1756 that flips-out, resembling the “pre-formed” unoccupied state of the DC in bacteria [9, 17]. Particularly, the tip of H69 points inside the DC, inducing the rearrangement of A1756 and most likely promoting the stacking of A2256 and A1755 (Figs. 2j and 3f). However, in contrast to (i) prokaryotic 70S/mRNA/2tRNAs complex with A-site unoccupied [9] and to (ii) pre-translocating 70S/mRNA/tRNA/EFG/GMPPCP complex [17, 18], we observe an additional interaction between A1756

and the mRNA backbone at position +5 (Fig. 3f). Our data suggest that sordarin impacts the conformation of the tip of domain IV of eEF2, and in turn diphthamide position, thus retaining the modification from interacting closely with h44 and the mRNA. The binding of sordarin constrains further eEF2 domain III, which in turn influences diphthamide position (Figs. 2 and 3, and Supplement Fig. 2c). This is in agreement with previous studies, where sordarin was shown to prevent domain III from moving away from the GTPase activating center of the sarcin–ricin loop, thereby avoiding dissociation of eEF2 from the ribosome and reverse rotation of SSU [5, 15, 23]. As it was indicated earlier, sordarin can stabilize one of the intermediate states of eEF2 before and after hydrolysis of GTP without interfering with its hydrolysis [10]. These findings support our interpretation of the “AIF₄/sordarin complex” structure, which most likely reflects post-hydrolysis events of translocation.

Structural role of diphthamide in ribosomal translocation in eukaryotes

Our reconstructions provide structural evidence of how diphthamide might be responsible for regulation of the molecular switch between major nucleotides of the DC, thus playing an active role in controlling mRNA movement on the ribosome. In addition, our reconstructions reveal that the conserved protein uS12, which also belongs to the DC and binds to domain III of eEF2 [15], contacts the backbone of A1755 and A1756 (Supplement Fig. 7a–c), likely stabilizing their conformation, similarly to that for bacteria [17].

The knowledge of the structural implication of diphthamide in the translocation of mRNA is very limited, and reconstructions, obtained in the same range of resolution as ours, are only available for 80S/eEF2/viral-IRESs, in the presence of either GMPPCP [19] or GDP + sordarin [15]. In the structure of yeast 80S/eEF2/GMPPCP/CrPV IRES (PDB code: 5it7) [19], the diphthamide is interacting with the codon–anticodon-like moiety of PKI in a way that prevents the decoding residues to bind the IRES. This is reminiscent of what we observed in the “GMPPCP complex,” where the conserved A1755/56 of the DC is positioned inside the minor groove of h44. However, in the fully rotated structure of 80S/eEF2/GDP/sordarin/TSV IRES complex (PDB code: 5juu [15]), diphthamide is pointing to the codon–anticodon-like helix of PKI, occupying the hybrid ap/P position, and interacts with the decoding residue A1756, similarly to what we observe in the case of the “AIF₄/sordarin complex.” We can therefore deduce that the position of diphthamide we observe in the presence of GDP + AIF₄ can be attributed to as a post-hydrolytic state. Finally, diphthamide in the “GMPPCP/sordarin” complex adopts a very unusual conformation as its position is not observed in any of the structures of 80S/eEF2/IRESs [15, 19].

Conclusions

In the present study, we provide novel structural evidence of the role of diphthamide in ribosomal translocation in the presence of mRNA and tRNA (Figs. 3 and 4). We suggest that this highly conserved post-translational modification of eEF2 enhances the fidelity of translation by ensuring correct reading frame of mRNA via direct interaction with it and with the rRNA in the DC (Figs. 2 and 3, and Supplement Fig. 4). These interactions might be needed to avoid possible back rotation of the SSU and/or mRNA slippage, which can result in mRNA frame-shift and lead to errors in polypeptide chain biosynthesis (Fig. 4) [24]. The interaction network established between the diphthamide and the DC appears to be dependent on the position of domain IV of eEF2 that in turn is dependent on the nucleotide state and other ligands such as sordarin. Appearance of diphthamide in the course of evolution might have been dictated by the more complex regulation level of the eukaryotic ribosome compared to bacteria [21], which required additional molecular tools to ensure accuracy of translocation, in order to avoid the spontaneous frame-shifting [24]. Although the insights gained about the structural role of diphthamide point toward its direct implication in reading frame maintenance, we still require thorough structural and functional investigations of other intermediates to understand entirely the mechanism of translocation and the full extent of the role played by the diphthamide in this process.

Materials and Methods

Ribosome and eEF2 purification

The 80S ribosome was purified accordingly to the previous protocol [22] with minor changes. One of the modifications of the published protocol was the addition of spermidine (2.5 mM) to sucrose density gradients at the moment of gradients formation. To overcome the problem of having stress protein factor Stm1 [22], which binds to major active sites of the 80S ribosome upon stress condition employed during ribosomes purification, we generated a new strain lacking the gene encoding for Stm1. *S. cerevisiae* strain JD1370- Δ Stm1 was obtained from strain JD1370 (MATa, ura3, leu2, pep4::HIS3, nuc1::LEU2, stm1::TRP1, L_A [22]) by replacing *stm1* gene with a TRP1 marker. The TRP1 marker was PCR generated using pBS2438 plasmid as a template, and TTTA GAGGTGAAGTAGAAATAACCAAGAAAGCATA CACATTTTATTCTCATccatggaaaagagaag and GTA GAACACTGTTATTGGATTCTTTTCAGTTGGAAT TATTCATATATAAGGCtacgactcactataggg as primers (capitalized are segments complementary to

stm1 gene locus). The isolation procedure of native eEF2 was mainly based on the protocol described earlier [7], where several steps were changed. Firstly, we used fresh culture of yeast strain JD1370- Δ Stm1 grown to an A_{600} of 2–3 and cells were lysed in a microfluidizer. Secondly, instead of S-Sepharose, source-Q and uno-Q ion-exchange columns, we used SP-Sepharose, Q-Sepharose and mono-Q columns and introduced a gel filtration with Superdex 200 as the final purification step.

The “GMPPCP complex” was formed in buffer G [10 mM Hepes–KOH, 5 mM Mg(OAc)₂, 40 mM KOAc, 10 mM NH₄Cl (pH 7.5)]. The eEF2/GMPPCP mixture was incubated for 30 min at room temperature before the addition to the mixture of 80S ribosomes (5 mg/mL, 1.125 μ M) with mRNA and tRNA added at 3-fold and 5-fold molar excesses, respectively, in two consecutive steps of 15 min each at 30 °C. The mRNA sequence used was (CAA)₅UUUUUUUUU, while the tRNA we employ was yeast tRNA^{Phe}. The factor mix was then incubated with the ribosomes, mRNA and tRNA for 30 min at 30 °C. The eEF2 factor was used at 3-fold excess over the ribosomes, and concentration of GMPPCP was 0.25 mM. Following the last incubation step, the mixture was sized on Superdex 200 column equilibrated in buffer G [22]. The ribosome complex was collected from the void volume, concentrated to 70 nM and used for preparation of the cryo-EM grids.

Complexes “AIF₄⁻/sordarin” and “GMPPCP/sordarin” were prepared in the similar way except that in the latter, 0.1 mM of sordarin was preincubated with the eEF2/GMPPCP mixture at room temperature for 30 min prior to the addition to the ribosome mix. In the case of the “AIF₄⁻/sordarin complex,” GDP was added to the eEF2 mix instead of GMPPCP at a final concentration of 0.2 mM with sordarin kept at 0.1 mM. In order to create the AIF₄⁻ group, AlCl₃ and NaF were added at final concentrations of 0.2 and 5 mM, respectively, to the eEF2/GDP/sordarin mix. Both complexes were sized on Superdex 200 and concentrated to 70 nM as described above.

Grids preparation and data collection parameters

The grids were prepared by applying 4 μ L of each complex at ~70 nM to 400 mesh holey carbon Quantifoil 2/2 grids (Quantifoil Micro Tools). The grids were blotted for 1.5 s at 4 °C, 100% humidity, using waiting time 30 s, and blot force 4 (Vitrobot Mark IV). The data acquisitions were performed on a Titan Krios S-FEG instrument (FEI) operated at 300-kV acceleration voltage and at a nominal under-focus of $\Delta z = -0.8$ to -4.5 μ m using the second-generation back-thinned direct electron detector CMOS (Falcon II) 4096 \times 4096 camera and automated data collection with EPU software (FEI). The Falcon II camera was calibrated at nominal magnification of 59,000 \times . The calibrated magnification on the

14- μm pixel camera is 127,272 \times , resulting in 1.1- \AA pixel size at the specimen level. The camera was set up to collect 8 frames and frames 2 to 8 were aligned. Total exposure was 1.5 s, with a dose of 60 $\text{e}^-/\text{\AA}^2$ (or 3.5 $\text{e}^-/\text{\AA}^2$ per frame).

Image processing

SCIPION [25–27] package was used for image processing and 3D reconstruction. Optical Flow algorithm integrated in Xmipp3 [28] was used for the movie alignment of ~1196 images from the GMPPCP complex, ~2030 images from the “AIF₄/sordarin” complex and ~3184 images for the GMPPCP/sordarin complex. CTFFIND4 [29] was used for the estimation of the contrast transfer function of an average image of the whole stack. The frame image motion for all three image data sets was corrected using Optical Flow (OF [27]). In the case of the “AIF₄/sordarin complex” data set, in addition to OF [27], we corrected the whole frame image motion using Motion_Corr [30] before particle picking/extraction and 3D classification, with no significant improvement on the resolution and the level of eEF2 interpretation. Particles were selected in SCIPION [31]. Approximately 150,000 particles were selected for the “GMPPCP complex,” 156,000 particles for the “AIF₄/sordarin complex” and 320,000 particles for the “GMPPCP/sordarin complex.” RELION [12] was used for particle sorting through 3D classification via SCIPION, (please refer to Supplement Fig. 1 for particle sorting details for all three complexes). Selected classes were refined using RELION's 3D autorefine and the final refined classes were then post-processed using the procedure implemented in RELION applied to the final maps for appropriate masking, *B* factor sharpening and resolution validation to avoid over-fitting [12], indicating an average resolution of 4.0 \AA for the “GMPPCP complex,” 3.9 \AA for the “AIF₄/sordarin complex” and 4.4 \AA for the “GMPPCP/sordarin complex” (Supplement Fig. 1 and Supplement Table 1). We afterward created two different masks: first mask focused on the SSU (including the tRNA, mRNA and eEF2) and a second mask focused on the LSU with the most stable regions of the SSU at the intersubunit side (including h44 and the P-site, tRNA, mRNA and eEF2). These masks were used for 3D auto-refine jobs in RELION [12]. The resulting reconstructions were then post-processed for automatic *B*-factor sharpening. The FSC curves corresponding to all the reconstructions performed in this work are shown in Supplement Fig. 1. The best resolutions obtained for the LSU-focused maps are 3.8, 3.7 and 4.3 \AA for the “GMPPCP,” “AIF₄/sordarin” and “GMPPCP/sordarin” complexes, respectively.

Segmentation and display of density maps

The cryo-EM maps were segmented by UCSF Chimera [32] using the SEGGGER module [33]. All the

segments counting fewer than 1000 voxels were discarded.

Local resolution measurement of the cryo-EM map

RESMAP [34] was used to estimate the local resolution of the cryo-EM reconstruction. The resolution was represented as a variable color scale using UCSF Chimera [32].

Model building and validation

The yeast 80S crystal structure (PDB: 4V88), the structure of eEF2 in GTP-like state bound to the ribosome (PDB: 2P8W) and the crystal structure of tRNA^{Phe} (PDB: 1EHZ) were initially docked as rigid bodies into the cryo-EM maps using Chimera [32]. Iterative cycles of manual building using Coot [35] and refinement (global and local) by phenix.real_space_refine [36] of the atomic coordinates were performed to improve the quality of the model and the fit into the electron density. RNA geometry was locally fixed using Erraser [37], from the Rosetta suite. The structures were finally validated using Molprobit [38] and the correlation coefficients were calculated using phenix.map_model_cc [36]. All the figures for the manuscript were prepared using Pymol (The PyMOL Molecular Graphics System, Version 1.7 Schrödinger, LLC.).

Accession numbers

The cryo-EM maps and atomic coordinates have been deposited in the EMDB and Protein Data Bank under accession codes EMD-0049 and PDB ID 6GQV, EMD-0048, EMD-0055 and PDB ID 6GQB and EMD-007 and PDB ID 6GQ1 for “GMPPCP complex,” “AIF₄/sordarin complex” and “GMPPCP/sordarin complex,” respectively.

Acknowledgments

This work was supported by the French National Research Agency (ANR-15-CE11-0021-01, to G.Y.); “Fondation ARC pour la recherche sur le cancer” (to G.Y.); La Fondation pour la Recherche Médicale (DBF20160635745), France (to S.P. and G.Y.); European Research Council advanced grant 294312 (to M.Y.); and the Russian Government Program of Competitive Growth of Kazan Federal University (to M.Y.). A special thanks to Dr. Carlos Oscar Sorzano and Dr. Pablo Conesa for the support and the use of resources of Instruct, a Landmark ESFRI project. We would like also to thank the High Performance Computing Center of the University of

Strasbourg (funded by the Equipex Equip@Meso project) for IT support. This work was supported by the ANR-14-ACHN-0024 grant @RAction program “ANR CryoEM80S” and benefits from funding from the state managed by the French National Research Agency as part of the Investments for the Future program (to Y.H.).

Appendix A. Supplementary data

Supplementary data to this article can be found online at <https://doi.org/10.1016/j.jmb.2018.06.006>.

Received 29 January 2018;

Received in revised form 11 May 2018;

Accepted 4 June 2018

Available online 7 June 2018

Keywords:

ribosome translocation;

cryo-EM;

eEF2;

diphthamide;

reading-frame maintenance

Present address: N. Demeshkina, Biochemistry and Biophysics Center, National Heart, Lung and Blood Institute, Bethesda, MD, USA.

Present address: S. Melnikov, Department of Molecular Biophysics and Biochemistry, Yale University, New Haven, CT 06520, USA.

Abbreviations used:

SSU, small ribosomal subunit; LSU, large ribosomal subunit; DC, decoding center; cryo-EM, cryo-electron microscopy.

References

- [1] J. Achenbach, K.H. Nierhaus, The mechanics of ribosomal translocation, *Biochimie* 114 (2015) 80–89.
- [2] C. Ling, D.N. Ermolenko, Structural insights into ribosome translocation, *elife* 7 (2016) 620–636.
- [3] C.M. Spahn, M.G. Gomez-Lorenzo, R.A. Grassucci, R. Jorgensen, G.R. Andersen, R. Beckmann, P.A. Penczek, J.P. Ballesta, J. Frank, Domain movements of elongation factor eEF2 and the eukaryotic 80S ribosome facilitate tRNA translocation, *EMBO J.* 23 (2004) 1008–1019.
- [4] J. Sengupta, J. Nilsson, R. Gursky, M. Kjeldgaard, P. Nissen, J. Frank, Visualization of the eEF2-80S ribosome transition-state complex by cryo-electron microscopy, *J. Mol. Biol.* 382 (2008) 179–187.
- [5] D.J. Taylor, J. Nilsson, A.R. Merrill, G.R. Andersen, P. Nissen, J. Frank, Structures of modified eEF2 80S ribosome complexes reveal the role of GTP hydrolysis in translocation, *EMBO J.* 26 (2007) 2421–2431.
- [6] P.A. Ortiz, R. Ulloque, G.K. Kihara, H. Zheng, T.G. Kinzy, Translation elongation factor 2 anticodon mimicry domain mutants affect fidelity and diphtheria toxin resistance, *J. Biol. Chem.* 281 (2006) 32639–32648.
- [7] R. Jorgensen, A. Carr-Schmid, P.A. Ortiz, T.G. Kinzy, G.R. Andersen, Purification and crystallization of the yeast elongation factor eEF2, *Acta Crystallogr. D Biol. Crystallogr.* 58 (2002) 712–715.
- [8] R. Schaffrath, W. Abdel-Fattah, R. Klassen, M.J. Stark, The diphthamide modification pathway from *Saccharomyces cerevisiae*—revisited, *Mol. Microbiol.* 94 (2014) 1213–1226.
- [9] L.B. Jenner, N. Demeshkina, G. Yusupova, M. Yusupov, Structural aspects of messenger RNA reading frame maintenance by the ribosome, *Nat. Struct. Mol. Biol.* 17 (2010) 555–560.
- [10] J.M. Dominguez, M.G. Gomez-Lorenzo, J.J. Martin, Sordarin inhibits fungal protein synthesis by blocking translocation differently to fusidic acid, *J. Biol. Chem.* 274 (1999) 22423–22427.
- [11] E. Salsi, E. Farah, D.N. Ermolenko, EF-G Activation by Phosphate Analogs, *J. Mol. Biol.* 428 (2016) 2248–2258.
- [12] S.H. Scheres, RELION: implementation of a Bayesian approach to cryo-EM structure determination, *J. Struct. Biol.* 180 (2012) 519–530.
- [13] E. Svidritskiy, A.F. Brilot, C.S. Koh, N. Grigorieff, A.A. Korostelev, Structures of yeast 80S ribosome–tRNA complexes in the rotated and nonrotated conformations, *Structure* 22 (2014) 1210–1218.
- [14] S. Mohan, J.P. Donohue, H.F. Noller, Molecular mechanics of 30S subunit head rotation, *Proc. Natl. Acad. Sci. U. S. A.* 111 (2014) 13325–13330.
- [15] P.D. Abeyrathne, C.S. Koh, T. Grant, N. Grigorieff, A.A. Korostelev, Ensemble cryo-EM uncovers inchworm-like translocation of a viral IRES through the ribosome, 2016 5.
- [16] A.H. Ratje, J. Loerke, A. Mikolajka, M. Brunner, P.W. Hildebrand, A.L. Starosta, A. Donhofer, S.R. Connell, P. Fucini, T. Mielke, P.C. Whitford, J.N. Onuchic, Y. Yu, K.Y. Sanbonmatsu, R.K. Hartmann, P.A. Penczek, D.N. Wilson, C.M. Spahn, Head swivel on the ribosome facilitates translocation by means of intra-subunit tRNA hybrid sites, *Nature* 468 (2010) 713–716.
- [17] Y. Chen, S. Feng, V. Kumar, R. Ero, Y.G. Gao, Structure of EF-G–ribosome complex in a pretranslocation state, *Nat. Struct. Mol. Biol.* 20 (2013) 1077–1084.
- [18] D.S. Tourigny, I.S. Fernandez, A.C. Kelley, V. Ramakrishnan, Elongation factor G bound to the ribosome in an intermediate state of translocation, *Science* 340 (2013) 1235490.
- [19] J. Murray, C.G. Savva, B.S. Shin, T.E. Dever, V. Ramakrishnan, I.S. Fernandez, Structural characterization of ribosome recruitment and translocation by type IV IRES, *elife* 5 (2016).
- [20] S. Liu, C. Bachran, P. Gupta, S. Miller-Randolph, H. Wang, D. Crown, Y. Zhang, A.N. Wein, R. Singh, R. Fattah, S.H. Leppla, Diphthamide modification on eukaryotic elongation factor 2 is needed to assure fidelity of mRNA translation and mouse development, *Proc. Natl. Acad. Sci. U. S. A.* 109 (2012) 13817–13822.
- [21] J. Zhou, L. Lancaster, J.P. Donohue, H.F. Noller, Crystal structures of EF-G–ribosome complexes trapped in intermediate states of translocation, *Science* 340 (2013) 1236086.
- [22] A. Ben-Shem, N. Garreau de Loubresse, S. Melnikov, L. Jenner, G. Yusupova, M. Yusupov, The structure of the eukaryotic ribosome at 3.0 Å resolution, *Science* 334 (2011) 1524–1529.

- [23] R. Jorgensen, P.A. Ortiz, A. Carr-Schmid, P. Nissen, T.G. Kinzy, G.R. Andersen, Two crystal structures demonstrate large conformational changes in the eukaryotic ribosomal translocase, *Nat. Struct. Biol.* 10 (2003) 379–385.
- [24] N. Caliskan, F. Peske, M.V. Rodnina, Changed in translation: mRNA recoding by –1 programmed ribosomal frameshifting, *Trends Biochem. Sci.* 40 (2015) 265–274.
- [25] C.O. Sorzano, M. Alcorlo, J.M. de la Rosa-Trevin, R. Melero, I. Foche, A. Zaldivar-Peraza, L. del Cano, J. Vargas, V. Abrishami, J. Oton, R. Marabini, J.M. Carazo, Cryo-EM and the elucidation of new macromolecular structures: Random Conical Tilt revisited, *Sci. Rep.* 5 (2015) 14290.
- [26] J.M. de la Rosa-Trevin, A. Quintana, L. Del Cano, A. Zaldivar, I. Foche, J. Gutierrez, J. Gomez-Blanco, J. Burguet-Castell, J. Cuenca-Alba, V. Abrishami, J. Vargas, J. Oton, G. Sharov, J.L. Vilas, J. Navas, P. Conesa, M. Kazemi, R. Marabini, C.O. Sorzano, J.M. Carazo, Scipion: a software framework toward integration, reproducibility and validation in 3D electron microscopy, *J. Struct. Biol.* 195 (2016) 93–99.
- [27] V. Abrishami, J. Vargas, X. Li, Y. Cheng, R. Marabini, C.O. Sorzano, J.M. Carazo, Alignment of direct detection device micrographs using a robust Optical Flow approach, *J. Struct. Biol.* 189 (2015) 163–176.
- [28] J.M. de la Rosa-Trevin, J. Oton, R. Marabini, A. Zaldivar, J. Vargas, J.M. Carazo, C.O. Sorzano, Xmipp 3.0: an improved software suite for image processing in electron microscopy, *J. Struct. Biol.* 184 (2013) 321–328.
- [29] A. Rohou, N. Grigorieff, CTFIND4: fast and accurate defocus estimation from electron micrographs, *J. Struct. Biol.* 192 (2015) 216–221.
- [30] X. Li, P. Mooney, S. Zheng, C.R. Booth, M.B. Braunfeld, S. Gubbens, D.A. Agard, Y. Cheng, Electron counting and beam-induced motion correction enable near-atomic-resolution single-particle cryo-EM, *Nat. Methods* 10 (2013) 584–590.
- [31] V. Abrishami, A. Zaldivar-Peraza, J.M. de la Rosa-Trevin, J. Vargas, J. Oton, R. Marabini, Y. Shkolnisky, J.M. Carazo, C.O. Sorzano, A pattern matching approach to the automatic selection of particles from low-contrast electron micrographs, *Bioinformatics* 29 (2013) 2460–2468.
- [32] E.F. Pettersen, T.D. Goddard, C.C. Huang, G.S. Couch, D.M. Greenblatt, E.C. Meng, T.E. Ferrin, UCSF Chimera—a visualization system for exploratory research and analysis, *J. Comput. Chem.* 25 (2004) 1605–1612.
- [33] G.D. Pintilie, J. Zhang, T.D. Goddard, W. Chiu, D.C. Gossard, Quantitative analysis of cryo-EM density map segmentation by watershed and scale-space filtering, and fitting of structures by alignment to regions, *J. Struct. Biol.* 170 (2010) 427–438.
- [34] A. Kucukelbir, F.J. Sigworth, H.D. Tagare, Quantifying the local resolution of cryo-EM density maps, *Nat. Methods* 11 (2014) 63–65.
- [35] P. Emsley, B. Lohkamp, W.G. Scott, K. Cowtan, Features and development of Coot, *Acta Crystallogr. D Biol. Crystallogr.* 66 (2010) 486–501.
- [36] P.V. Afonine, J.J. Headd, T.C. Terwilliger, P.D. Adams, *Comput. Crystallogr. Newsl.* 4 (2013) 43–44.
- [37] F.C. Chou, P. Sripakdeevong, S.M. Dibrov, T. Hermann, R. Das, Correcting pervasive errors in RNA crystallography through enumerative structure prediction, *Nat. Methods* 10 (2013) 74–76.
- [38] V.B. Chen, W.B. Arendall 3rd, J.J. Headd, D.A. Keedy, R.M. Immormino, G.J. Kapral, L.W. Murray, J.S. Richardson, D.C. Richardson, MolProbity: all-atom structure validation for macromolecular crystallography, *Acta Crystallogr. D Biol. Crystallogr.* 66 (2010) 12–21.